Journal of Polymer Science

WILEY

JOURNAL OF POLYMER SCIENCE

RESEARCH ARTICLE OPEN ACCESS

Vegetable Oil–Mediated Transesterification as a Green Route to Tune Ethyl Cellulose Properties

Athira Narayanan[1] | Valeria D'Errico[1] | Marco Friuli[1] | Sonia Bagheri[1] | Claudio Mele[1] | Alessandro Sannino[2] | Christian Demitri[2] | Leonardo Lamanna[1,2]

[1]Department of Engineering for Innovation, University of Salento, Lecce, Italy | [2]Department of Experimental Medicine, University of Salento, Lecce, Italy

Correspondence: Athira Narayanan (athira.narayanan@unisalento.it) | Leonardo Lamanna (leonardo.lamanna@unisalento.it)

Received: 24 October 2025 | **Revised:** 3 February 2026 | **Accepted:** 15 February 2026

Keywords: chemical modification | ethyl cellulose | green synthesis | hydrophobization | renewable material | transesterification | transparent surface coating

ABSTRACT

The inherent hydrophilicity of biopolymers presents significant limitations to their implementation, particularly in coating and packaging applications. Concerns regarding the toxicity, cost, and environmental impact of conventional chemical strategies for hydrophobization have prompted researchers to pursue more sustainable and eco-friendlier approaches. This study centers on a solvent-free, green, transesterification reaction (TER) to chemically graft fatty acid ethyl esters derived from diverse vegetable oils onto ethyl cellulose (EC), yielding enhancements in hydrophobicity, flexibility, and barrier performance without synthetic reagents. Successful TER of EC was verified through Fourier transform infrared spectroscopy. Among the tested oils, sunflower oil exhibited the highest TER efficiency (> 25%), attributable to high polyunsaturated fatty acid content. Atomic force microscopy confirmed a homogeneous surface morphology for TER-modified EC, while mechanical analysis revealed a threefold enhancement in elongation at break compared to unmodified EC. Moreover, oxygen and water vapor transmission rates were reduced by ~50%, signifying improved barrier properties. TER enhanced optical transparency (~82%) and surface hydrophobicity (~97°) for EC, as well as displayed better performance as a coating on substrates like wood. Integrating renewable feedstock into the TER protocol provides a potent pathway for sustainable chemical modification of EC while minimizing environmental impact by adhering to green chemistry principles.

1 | Introduction

The development of hydrophobic systems is of significant interest in various sectors, including the packaging industry, textiles, water purification, electronics, natural stone preservation, biomedical applications, and other areas where moisture resistance plays a crucial role [1]. Their desirable water-repellent properties also confer anti-corrosion, self-cleaning, moisture barrier, anti-freezing, anti-icing, and anti-adherence properties [2, 3]. Synthetic materials, such as fluorinated polymers and organosilanes, have been widely explored as the gold standard for improving hydrophobicity [4, 5]. Fluorinated polymers are well known for their excellent water and oil repellency, which is attributed to their very low surface energy, which significantly extends the shelf life of perishable products [6]. The high costs of these materials pose significant challenges in fabrication and raise concerns owing to their links to immunotoxicity, adverse health effects, and environmental persistence [1, 7]. Organosilanes, another class of materials, offer a versatile option for creating durable

Abbreviations: AFM, atomic force microscopy; ATR-FTIR, attenuated total reflectance—Fourier transform infrared spectroscopy; CA, contact angle; EAB, elongation at break; EC, ethyl cellulose; FA, fatty acid; FAEE, fatty acid ethyl ester; OTR, oxygen transmission rate; R_{TER}, relative transesterification reaction rate; TER, transesterification reaction; UTS, ultimate tensile strength; WVTR, water vapor transmission rate; YM, young's modulus.

hydrophobic surfaces through chemical bonding with substrates [8, 9]. Despite their low cost, effectiveness, and relatively lower toxicity, their application is often hindered by complex processing and the risk of chemical leaching [10]. Polysiloxanes, another class of organosilicon compounds, exhibit enhanced water resistance compared to higher-alkane compounds because of their lower surface energies. However, their environmental compatibility is still debated, requiring controlled applications to mitigate impacts [11]. Finding a balance between the advantages of materials and their ecological consequences is vital, prompting researchers to seek new, more environmentally friendly, and cleaner options.

Natural polysaccharides, such as starch, cellulose, chitin, and chitosan, have been extensively studied as substitutes for synthetic coating materials because of their non-toxicity, biocompatibility, and biodegradability [12–15]. The use of biopolymers as coating materials is generally limited by their hydrophilic nature, which reduces their effectiveness as protective barriers [16]. For example, alginate or chitosan (among the most studied), when applied as a coating on cardboard employed for packaging, presented a hydrophilic behavior, with contact angles of ~50° [17, 18]. In addition to these properties, transparency is another crucial feature, as it enables the assessment of features, quality, and contents of products, while being essential for optical applications requiring specific wavelengths within the visible spectrum [19–22]. Therefore, the pursuit of alternatives to synthetic polymers, modifications to biopolymers, and innovative chemical modification strategies requires concentrating on viable solutions that uphold these essential properties [23].

Ethyl cellulose (EC), a cellulose derivative, is a promising candidate in this context because of its slightly hydrophobic nature, owing to the presence of ethoxy (CH_3CH_2—) groups. Despite its non-toxicity, biodegradability, and cost-effectiveness, this material has been little explored because it becomes non-transparent and exhibits poor mechanical properties (e.g., brittleness) when dissolved in green solvents such as ethanol [24]. EC has been investigated for its water-resistant properties in surface coatings in the medical field and packaging, particularly when combined with other materials [25–27]. However, their performance in standalone applications has been limited by a lack of compactness and overall efficiency [28]. Only a few studies have investigated EC modifications via silanisation, acylation, fluorination, grafting, and esterification to improve hydrophobicity. However, these modifications depend extensively on toxic solvents and elaborate multi-step procedures, which undermine their environmental sustainability with the production of hazardous waste and significantly impair the material's intrinsic biodegradability by integrating durable synthetic components [29–31]. Lamanna et al. (2024) reported the development of a bioplastic, “OleoPlast”, using EC-based oleogels. Despite promising results, these materials exhibit contact angles of 70°–90° and are not well-suited for coating applications because of their high processing temperatures and low compatibility with solvents that disrupt their three-dimensional structure [32, 33].

Recently, the transesterification reaction (TER) has garnered considerable attention as a strategy for modifying biopolymers, owing to its simplicity, efficiency, and minimal equipment requirements [34, 35]. Moreover, it has already been successfully applied in large-scale processes such as biodiesel production and the synthesis of polysaccharide esters [36]. This reversible organic reaction involves the exchange of one ester's alkoxy group with another. The heterogeneous/base-catalyzed TER strategy is widely employed not only due to its cost-effectiveness and lower corrosiveness, but also because it follows green principles from the point of view of atom economy, waste reduction, reusability, and safety [37, 38]. The use of large, bulky alkyl-chain-containing hydrocarbon compounds in TER has been explored for its potential to enhance polymer hydrophobicity, as the aggregation induced by them can hinder the hydroxy groups from forming hydrogen bonds with water [39–41]. In cellulose, TER occurs at approximately 110°C and is influenced by time and catalyst concentration [42, 43]. Although TER using fatty acid esters derived from various oils has been widely explored as a modification strategy to enhance the mechanical properties, barrier performance, and hydrophobicity of cellulose, the persistent reliance on toxic solvents in producing cellulose fatty acid esters poses a major obstacle to achieving scalable green synthesis [39, 44, 45].

This study investigated the chemical modification of EC with fatty acid ethyl esters (FAEEs) derived from vegetable oils via a simple thermochemical TER, aimed at enhancing its hydrophobicity and flexibility. The TER process facilitates the substitution of the —OH groups of EC with hydrophobic acyl chains (—COOR) of FAEEs, which can effectively enhance the hydrophobicity of EC. Additionally, the influence of fatty acid composition on TER rate was examined for peanut, sunflower, and soybean oils, the most prevalent and globally distributed commercial oils. The TER-modified EC was characterized from chemical, physical, and mechanical perspectives to evaluate its properties. Furthermore, this study explored the potential of the transesterified EC as a transparent coating for various surfaces, including glass, paper, cardboard, and wood. The utilization of renewable resources, such as vegetable oils and EC, in conjunction with the TER process, represents an innovative and sustainable hydrophobization strategy that embodies several core principles of green chemistry developed by Paul Anastas and John Warne, including waste prevention, safer auxiliaries and solvents (employing ethanol for FAEE preparation and solvent-free grafting onto the EC backbone), mild reaction conditions, utilization of renewable feedstocks, and minimal catalysis [46, 47]. This methodology not only enables the development of advanced bio-based hydrophobic materials but also drives substantial progress toward sustainable innovations in materials science.

2 | Results and Discussion

The chemical modification of EC was achieved through the TER, using FAEEs derived from vegetable oils. Initially, the vegetable oil underwent TER with ethanol (Scheme 1-1), generating FAEEs, which were subsequently used to transesterify the EC (Scheme 1-2). The TER mechanism of vegetable oil involves the formation of di- and monoglycerides as intermediates, producing three different FAEEs and glycerol as by-products, as reported in the literature [24]. In the subsequent step, with the

heat treatment at 110°C, the free —OH groups of EC were replaced with the —COOR groups of FAEEs, resulting in the production of fatty acid esters of EC.

2.1 | Attenuated Total Reflectance—Fourier Transform Infrared Spectroscopy (ATR-FTIR)

The FTIR spectra of the EC, vegetable oils, and transesterified EC with FAEEs of three different vegetable oils are portrayed in Figure 1A–C, and their characteristic peaks are presented in Table 1. The distinct ester carbonyl (—C═O) absorption band in the range 1738–1736 cm^{-1}, shifted from the typical ester carbonyl peak of pure vegetable oils, 1743–1742 cm^{-1}, has been observed, which indicates the successful TER of EC with FAEEs [48]. The shift in ester carbonyl peaks occurred because of the change in the chemical environment surrounding the —C═O bond after the TER [49]. Furthermore, the rise of a peak at 2921 cm^{-1}, corresponding to the aliphatic chain stretching of the vegetable oil, further confirms the successful TER [44].

The relative transesterification reaction rate, R_{TER}, reflects the rate of fatty acid esters production. An increase in the R_{TER} was observed with the heat treatment time at 110°C, accompanied by a corresponding enhancement in the peak intensity of the new C═O ester carbonyl peak. Among the vegetable oil-derived FAEEs, the maximum R_{TER} toward EC followed the order: sunflower oil > soybean oil > peanut oil (Figure 1D). The FAEEs of sunflower oil showed a higher rate of ~28% at 120 min compared to other vegetable oil-derived FAEEs. No significant increase in the R_{TER} was observed after 120 min of heat treatment at 110°C (Figure S1), and a decrease in the R_{TER} after 120 min suggests the hydrolysis or degradation of the EC backbone or FAEEs [44]. FTIR in ATR mode is generally considered less effective than transmission measurements due to penetration depth and contact effects [50]. Nevertheless, the present results demonstrate the robustness of this technique for evidencing the TER of EC with FAEEs of vegetable oils, with statistically significant differences confirmed by ANOVA (Figure S2).

The variability in R_{TER} as a function of heat treatment time is intrinsically linked to the composition of the vegetable oils. Predominant fatty acids (FAs) in vegetable oils typically include linoleic acid (C18:2), oleic acid (C18:1), stearic acid (C18:0), and palmitic acid (C16:0) [51]. Unsaturated fatty acids (linoleic and oleic acids) exhibit elevated reactivity compared to saturated analogues (palmitic and stearic acids) owing to the presence of double bonds [52]. Saturated FAs exhibit dense packing owing to strong London dispersion forces, which confer thermodynamic stability. Meanwhile, the *cis*-double bonds in the unsaturated FAs can introduce kinks in the hydrocarbon tails by reducing the interaction between the π orbitals. This could hinder the approach of the sp^2 atoms from the double bonds of neighboring chains, causing these neighboring chains to be more distant in unsaturated than saturated FAs. Consequently, the weakened London forces between the chains lead to a loosely packed arrangement, reducing steric hindrance and enhancing overall reactivity. This aligns with the lower viscosity of unsaturated FAs, which is inversely proportional to both chain length and the degree of saturation [53–56]. Taking into account the higher overall percentage of unsaturated FAs, particularly linoleic acid, sunflower oil has been reported to have a superior profile [57, 58]. Thus, the elevated levels of polyunsaturated FAs in sunflower oil contributed to the high R_{TER}, whereas the low R_{TER} was attributed to the high monounsaturated FAs in peanut oil. Therefore, EC transesterified with FAEEs derived from sunflower oil was selected for further characterization and it is hereafter referred to as TER-modified EC.

2.2 | Mechanical Properties

The mechanical properties of both unmodified and TER-modified EC films were analyzed and are reported in Figure 2A–D. The TER-modified EC film exhibited lower ultimate tensile strength (UTS) and Young's modulus (YM) but

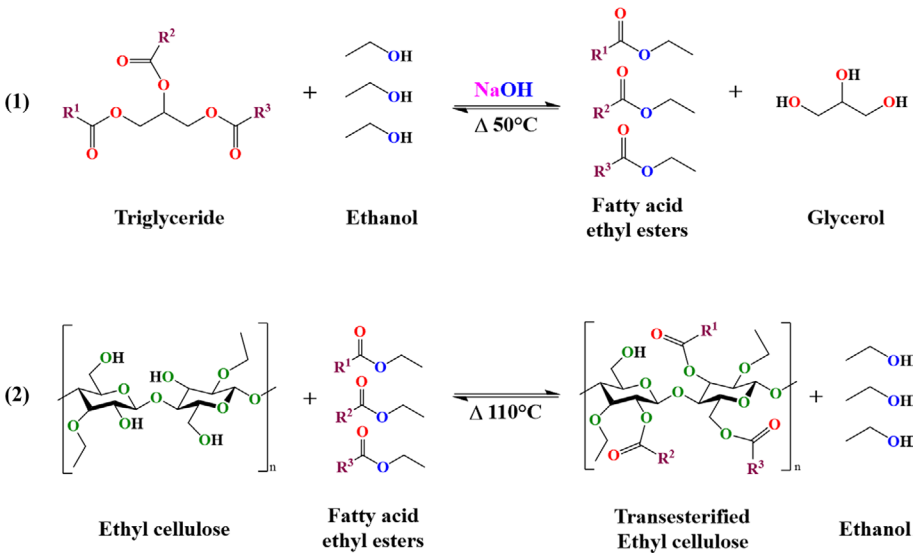

SCHEME 1 | The base-catalyzed transesterification reaction (TER) between (1) vegetable oil and ethanol at 50°C in the presence of NaOH catalyst, producing fatty acid ethyl esters (FAEEs) and glycerol, and (2) ethyl cellulose (EC) and FAEEs at 110°C, producing fatty acid esters of EC.

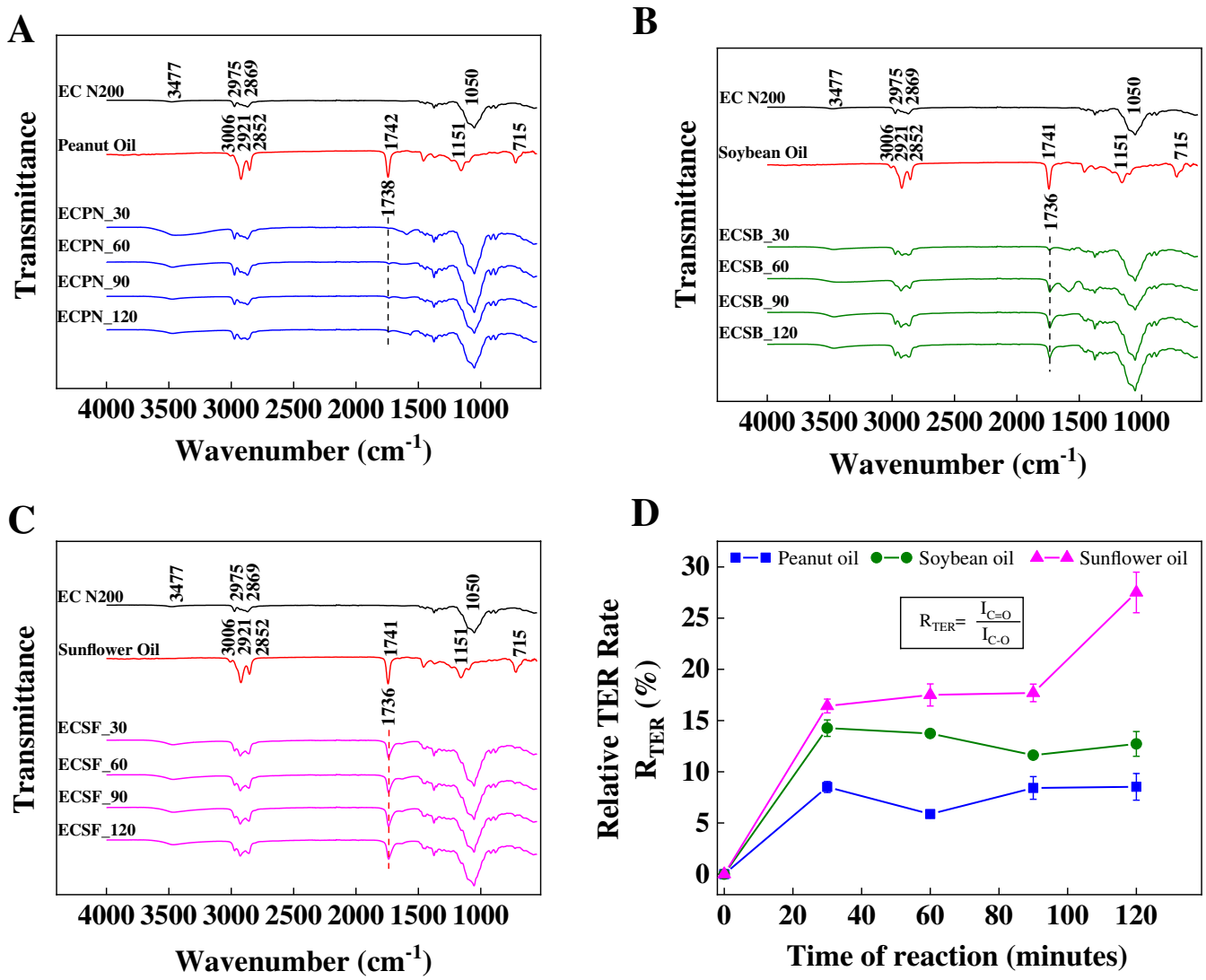

FIGURE 1 | The FTIR spectra of ethyl cellulose (EC) transesterified at 110°C for different heat treatment times (0, 30, 60, 90, and 120 min) with fatty acid ethyl esters (FAEEs) of (A) peanut oil (ECPN), (B) soybean oil (ECSB), (C) sunflower oil (ECSF), and (D) the relative TER rate (R_{TER}) of transesterified EC with FAEEs of three different vegetable oils with respect to the reaction time at 110°C calculated by the peak intensity ratio between the new ester carbonyl —C═O ($I_{C=O}$) peak in the range of ~1738–1736 cm^{-1} and —C—O (I_{C-O}) stretching bond of EC at ~1050 cm^{-1}.

a higher elongation at break (EAB) than the control unmodified EC film. The changes in the mechanical properties of the TER-modified EC film were attributed to the successive TER between EC and FAEEs. Following the TER, the modified film demonstrated an increase in elongation at break from 3.31% ± 0.21% to 8.24% ± 1.29%, confirming the potential of the TER in enhancing the flexibility of EC films. The observed UTS and YM for the TER-modified EC were 22.71 ± 3.44 MPa and 8.44 ± 0.63 MPa, respectively.

EC films are known for their brittleness due to the strong intermolecular hydrogen bonding between the polymer chains, which arises from the "active centers", leading to the formation of a three-dimensional structure when dried [59]. This TER process disrupted the intermolecular interactions in EC and generated new ester carbonyl (—C═O) bonds between the constituents, which exhibit greater mobility and enhanced plastic deformation. The presence of FAEE chains in the EC polymer matrix reduces the number of active centers available and impedes polymer aggregation, consequently weakening the interactions between polymer chains. This diminishes the three-dimensional structure and allows film deformation [60].

2.3 | Atomic Force Microscopy (AFM)

The AFM topographical images of unmodified EC and TER-modified EC samples are presented in Figure 3. While both surfaces appear generally smooth at the micrometric scale, morphological differences can be observed. The unmodified EC sample reveals a granular surface morphology. In contrast, the TER-modified EC displays a more homogeneous morphology, characterized by a largely featureless surface, suggesting that the modification process leads to a more uniform surface arrangement through the reduction of grain structures associated with hydrogen-bonded domains.

TABLE 1 | FTIR spectra of EC, vegetable oils, and TER-modified ECs.

Materials	Wavenumber (cm^{-1})	Vibration	References
EC	3477	—OH stretching	[24, 32]
	2975 and 2869	Asymmetric and symmetric —CH stretching, respectively	
	1050	Symmetric —C—O—C stretching	
Vegetable oils	3006	Symmetric C—H stretching of olefinic double bonds	[24, 32]
	2921 and 2852	Asymmetric and symmetric stretching vibration of the C—H of aliphatic CH_2 groups respectively	
	1744–1743	—C═O stretching of ester carbonyl groups of triglycerides	
	1151	—C—O stretching of the ester group	
	715	Out-of-plane vibration of cis-configured di-substituted olefins with the overlapping of the CH_2 rocking vibration	
TER modified ECs	2917 and 2926	Asymmetric stretching vibration of C—H of aliphatic CH_2 groups from triglyceride	Present work
	1738–1736	—C═O stretching of ester carbonyl groups of fatty acid esters of EC (after heat treatment at 110°)	
	1050	Symmetric —C—O—C stretching	

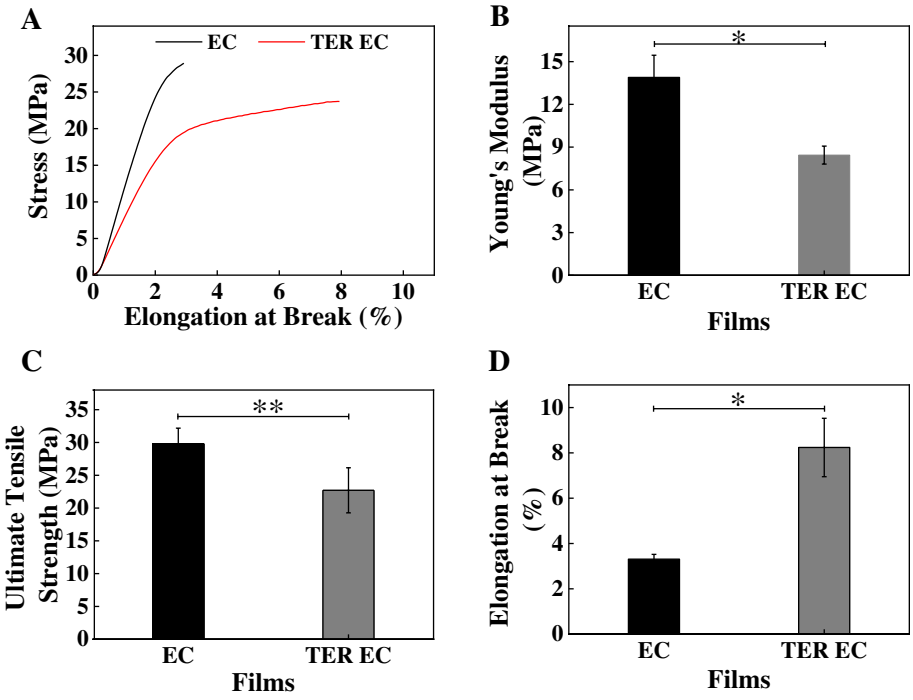

FIGURE 2 | The mechanical properties of EC and TER-modified EC (represented as TER EC) films are (A) the stress–strain graph, (B) Young's modulus, (C) ultimate tensile strength, and (D) elongation at break. *$p < 0.05$, **$p < 0.01$.

The quantitative R_a and R_q roughness parameters evaluated in triplicate over an area of $5 \times 5\,\mu m^2$ are summarized in Table 2. A comparison of these values shows only minor variations between the two samples, indicating that the TER modification does not significantly affect the overall surface roughness. This suggests that the TER technique primarily alters surface chemistry and morphology without inducing substantial changes in surface roughness.

2.4 | Permeability

The measured oxygen transmission rate (OTR) values were $4054 \pm 5\,cc/m^2/day$ for EC and $2086 \pm 6\,cc/m^2/day$ for TER-modified EC, while the water vapor transmission rate (WVTR) values were $291 \pm 7\,g/m^2/day$ for EC and $151 \pm 5\,g/m^2/day$ for TER-modified EC (Figure 4A,B). These results indicate that the OTR and WVTR of the TER-modified EC are approximately

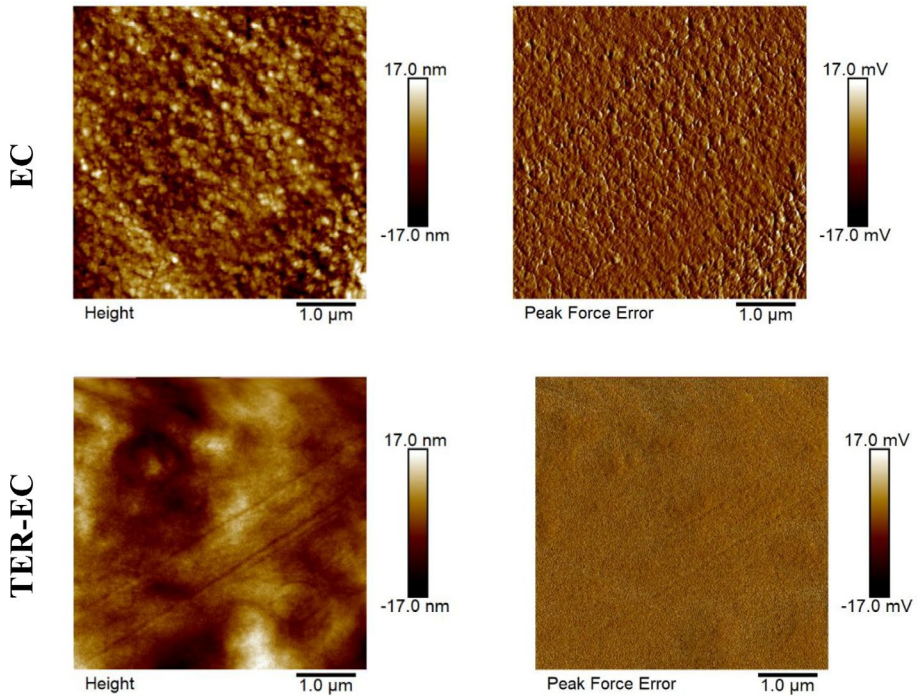

FIGURE 3 | AFM images showing height and peak-force errors of EC and TER-modified EC film (represented as TER-EC) samples.

TABLE 2 | Roughness values of the samples extracted from the AFM topographic images.

Sample film	Roughness (nm)	
	R_q	R_a
EC	4.56 ± 0.28	3.58 ± 0.25
TER-modified EC	5.23 ± 0.72	3.65 ± 0.57

50% lower than those of the control unmodified EC with the same thickness (~100 µm), highlighting the enhanced barrier properties through the TER. The obtained OTR and WVTR values for the TER-modified EC fell below the common range for bioplastics (OTR: < 5 kcc/m^2/day and WVTR: < 400 g/m^2/day), indicating its suitability for packaging applications [32].

The olefinic hydrophobic chains resulting from the FAEEs contributed to the enhancement of barrier qualities, and similar attributes were noted for polyolefins [61]. These results demonstrate that the TER process, which involves introducing alkyl chains into EC, facilitates improved water and oxygen barrier properties. This improvement is ascribed to the amplified hydrophobic contribution of the EC backbone, making the material potentially suitable for packaging applications [61, 62].

2.5 | Water Contact Angle Measurement

The water contact angle measurements on pure films revealed an increase of approximately 25% for the TER-modified EC film, from 78.46° ± 1.22° to 97.36° ± 2.76°, confirming the TER as a successful surface hydrophobization method for EC (Figure 4Ci). Additionally, the contact angle (CA) assessments on four distinct surfaces coated with unmodified EC and TER-modified EC solutions demonstrated their water-repellent properties (Figure 4Cii). An increase in CA was observed for all the TER-modified EC-coated surfaces. The control samples for tissue paper and wood exhibited a zero-contact angle, indicating complete wettability due to water absorption. For glass and tissue paper, the contact angles showed no significant difference between the unmodified and the TER-modified EC-coated samples. While the TER-modified EC coated on wood and cardboard surfaces exhibited a significant increase, measuring 93.15° ± 0.79° and 87.75° ± 0.40°, respectively.

The inherent roughness and surface energy of these materials may overshadow the effects of the coating's chemical composition, thereby minimizing any noticeable differences in hydrophobicity as reflected by the contact angle measurements [23]. The enhanced hydrophobicity observed on the wood surface due to the TER-modified EC coating, attributed to the strong affinity of fatty acid chains (a characteristic also exploited by oils commonly used to "revive" wood), and suggests the potential for developing transparent water-repellent coatings [63].

2.6 | UV–Vis Spectrophotometry

The UV–Vis spectroscopic analysis assessed the optical transmittance of lab glass slides coated with unmodified EC and TER-modified EC, and the substrate's transparency is shown in Figure 5A. This simple test demonstrates that the TER-modified EC coating exhibits transparency, allowing the university logo to be seen under the glass slide, unlike the unmodified EC-coated glass, which appears opaque and obscures the underlying details. The thickness of the coating was about ~150 µm as measured by the Dino Lite microscope. In the visible spectrum (> 380 nm), the bare glass surface exhibited a

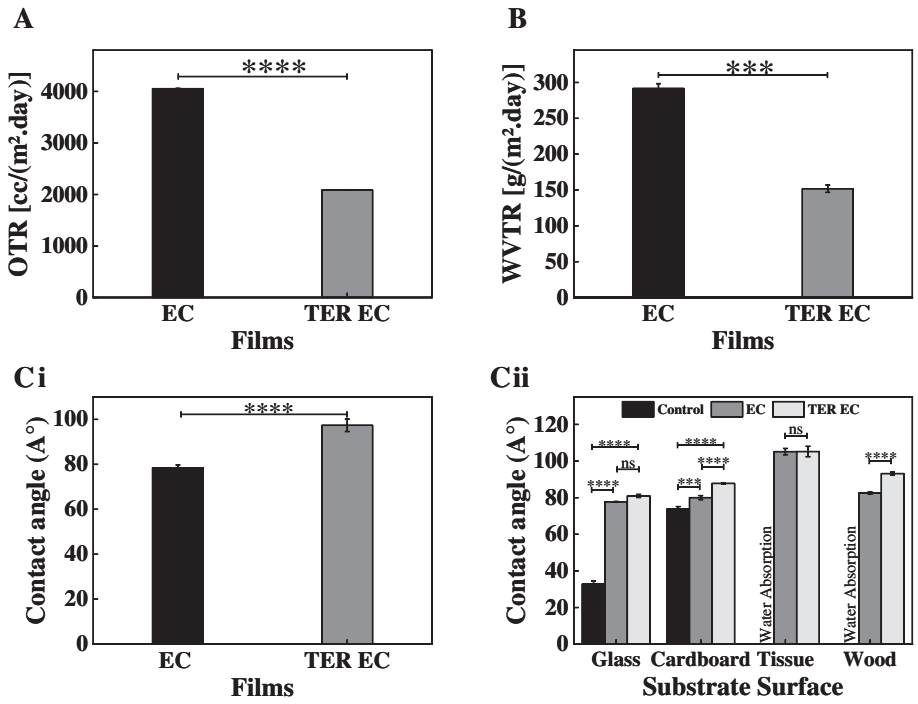

FIGURE 4 | The Permeability and contact angle analysis of EC and TER-modified EC (represented as TER EC). (A) The oxygen transmission rate, OTR, (B) the water vapor transmission rate, WVTR, and (C) contact angle measurements (i) for pure (non-coated) films and (ii) for coated substrate surfaces. ns, not significant, ***$p < 0.001$, ****$p < 0.0001$.

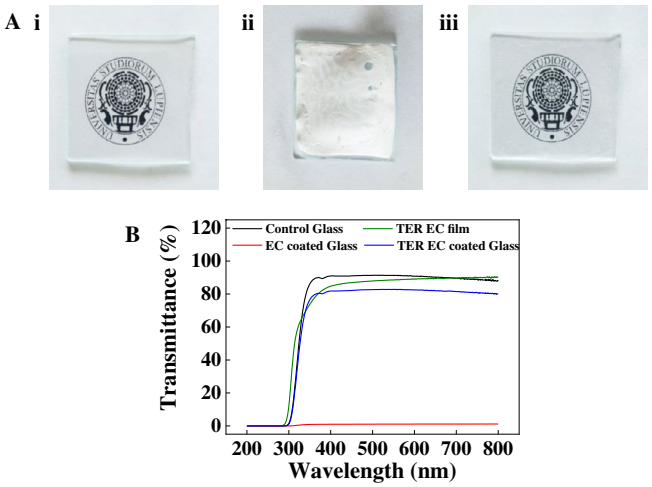

FIGURE 5 | The UV–Vis spectroscopic analysis on the lab glass slide coated with both EC and TER-modified EC (represented as TER EC), (A) the transparency comparison of the lab glass slide with the university logo, (i) uncoated, (ii) EC coated, and (iii) TER-modified EC coated, and (B) the transmittance analysis through the lab glass slide surface.

transmittance of approximately 91% ± 0.8%, whereas the TER-modified EC-coated glass showed a reduced transmittance of ~83% ± 1.5% (Figure 5B). In contrast, the unmodified EC-coated glass surface displayed an observable opacity with only 1.18% ± 0.1% transmittance. Notably, the 100 μm pure TER-EC film exhibits a transmittance profile very similar to that of glass, with a slight ability to transmit light at shorter wavelengths (287 nm). While the coating shows a slightly lower value of transmittance, likely due to optical interference effects occurring in the TER-modified EC coating–glass interface, where the phase difference depends on the coating's thickness and refractive index [64]. In addition, the presence of alkyl chains in TER-modified EC promotes the molecular rearrangement of EC, enhancing its compatibility with ethanol, which is traditionally considered a poor solvent for EC (usually dissolved in a mixture of ethanol and toluene). An increase in the solubility of TER-modified EC in ethanol reduces the coffee-stain effect, responsible for the opacity of EC-coated surfaces [65, 66].

3 | Conclusion

In this study, we developed a green transesterification strategy to enhance the hydrophobicity, flexibility, and barrier properties of EC using FAEEs derived from vegetable oils. Among the tested oils, sunflower oil exhibited the highest TER efficiency (28%), likely due to its higher polyunsaturated fatty acid content. Successful grafting of FAEEs onto the EC backbone was confirmed by FTIR analysis through the appearance of new ester carbonyl peaks.

The TER-modified EC demonstrated enhanced mechanical properties, with an elongation at break increased nearly threefold compared to that of unmodified EC. This improvement is attributed to the disruption of intermolecular hydrogen bonds in EC and the formation of new ester bonds during the TER reaction. AFM analysis revealed comparable surface roughness values but a more homogeneous morphology for TER-modified EC, in contrast to the granular surface of unmodified EC, indicating effective surface restructuring induced by the modification. Additionally, TER-modified EC exhibited superior water vapor

and oxygen barrier properties with approximately 50% reduction in both OTR and WVTR values and achieved significant transparency (~83% in the visible spectrum), compared to unmodified EC (opaque). The increased water contact angle (97°) confirmed its enhanced hydrophobic properties and demonstrated an improved transparent coating ability on wood substrates.

These laboratory-scale results provide proof of concept, illustrating how TER-modified EC can simultaneously enhance multiple functional properties through a simple, environmentally benign chemical modification. While promising, further research is required to evaluate the long-term durability and environmental stability of the modified films under realistic operating conditions, refine reaction kinetics for reproducible scalability, and undertake rigorous lifecycle analyses alongside biodegradability testing. Such advancements are essential to bridge persistent gaps between laboratory demonstrations and viable industrial applications, as commonly encountered in material innovations.

4 | Experimental Section

4.1 | Materials

Ethyl cellulose, EC N200 Aqualon with 48%–49.5% ethoxy content, was purchased from Ashland (Wilmington, USA). Absolute ethanol 99.9% (CH_3CH_2OH) and sodium hydroxide (NaOH) pellets were obtained from Sigma Aldrich (St. Louis, USA). Sunflower, soybean, and peanut oils were purchased from a local supermarket, specifically the Desantis brand oil. Peanut oil consists of 19% saturated fatty acids, 53% monounsaturated fatty acids, and 28% polyunsaturated fatty acids. Soybean oil comprises 15% saturated fatty acids, 24% monounsaturated fatty acids, and 61% polyunsaturated fatty acids. Sunflower oil contains 12% saturated fatty acids, 32% monounsaturated fatty acids, and 56% polyunsaturated fatty acids. All reagents were used without purification.

4.2 | Synthesis

The synthesis of transesterified EC involves the execution of two subsequent TERs. Initially, the TER of different vegetable oils was performed with ethanol at 50°C to produce their respective fatty acid ethyl esters (FAEEs) [24]. The produced FAEEs were then combined with a 3% EC solution (EC dissolved in absolute ethanol) and stirred overnight at 400 rpm and 50°C. This solution was drop-cast onto a Petri dish and dried at 50°C to obtain films. The EC to vegetable oil concentration ratio was maintained at 1:1. These dried films were further subjected to heat treatment at 110°C in an oven to carry out the TER of EC with the FAEEs for different time intervals: 30, 60, 90, and 120 min [67]. Following heat treatment, all samples were first washed for 2 h with distilled water to remove any water-soluble by-products, then dried at room temperature, and washed again with hexane for 2 h to eliminate apolar contaminants, such as free fatty acids and excess oil.

4.3 | Film Preparation and Surface Coating

To perform the coating tests, the dried TER-modified EC (0.75 g) was redissolved in 25 mL of absolute ethanol. As a control, an unmodified EC was prepared by dissolving 0.75 g EC in 25 mL of absolute ethanol. The TER-modified and unmodified EC solutions were selected to coat four different surfaces: glass, tissue paper, cardboard, and wood. Approximately 400 μL of each solution was coated onto these surfaces and allowed to dry at room temperature. In parallel, TER-modified EC films with a thickness of ~100 μm were produced for mechanical and permeability analysis using the drop-cast solvent evaporation method at 50°C. Approximately 25 mL of TER-modified EC solution was drop-cast into a Petri dish and dried at 50°C. Similarly, an unmodified EC film having the same thickness was produced as a control. The thickness of the films was measured using a Dino-Lite digital microscope (Taiwan, China).

4.4 | Characterizations

4.4.1 | Attenuated Total Reflectance—Fourier Transform Infrared Spectroscopy (ATR-FTIR)

The FTIR analysis was performed on the transesterified EC produced with FAEEs of different vegetable oils to assess the fingerprint region using a Jasco FT/IR-6300 spectrometer with an ATR PRO ONE X attachment (Easton, MD, USA) in the range of 4500–450 cm^{-1} with a resolution of 4 cm^{-1}. The relative TER rate, R_{TER} (%), was calculated from the peak intensity ratio between the new ester carbonyl —C═O ($I_{C=O}$) peak of fatty acid esters of EC (in the range 1738–1736 cm^{-1}) and —C—O (I_{C-O}) stretching bond of EC at ~1055 cm^{-1} using the following Equation (1) [67, 68].

$$Rate\ of\ transesterification(\%) = R_{TER} = \frac{I_{C=O}}{I_{C-O}} \quad (1)$$

Using the FTIR data, the R_{TER} for all EC, transesterified with FAEEs of different vegetable oils was calculated. The sample exhibiting the highest R_{TER} was identified and selected as the optimized TER-modified EC. The selected samples were then subjected to further comprehensive characterization.

4.4.2 | Tensile Strength Measurement

The mechanical properties of films were evaluated at a lab-controlled room temperature (25°C) using uniaxial tensile testing with dog bone-shaped specimens following ASTM D638 Type V by employing a Zwick/Roell universal testing machine. A velocity of 10 mm/min was applied within a 100 N load cell. No specific preconditioning was applied before the film characterization. The thicknesses of the films were measured before the mechanical test using a Dino-Lite digital microscope (Taiwan, China).

4.4.3 | Atomic Force Microscopy (AFM)

Atomic Force Microscopy (AFM) was utilized to characterize the surface topography and quantify the roughness of the samples investigated. Measurements were performed in triplicate using a Bruker MultiMode 8 system operating in PeakForce Quantitative Nanomechanical Mapping (QNM)

mode, which enabled the acquisition of high-resolution morphological images along with reliable roughness parameters. Scans were collected over an area of $5 \times 5\,\mu m^2$ at a scanning frequency of 0.85 Hz. A RTESPA-300 probe (Bruker), featuring a nominal resonance frequency of about 300 kHz and a force constant of 40 N/m, was used for all measurements. The acquired data were analyzed using Nanoscope Analysis software, version 1.5.

4.4.4 | Permeability Analysis

A Multi Perm Oxygen and Water Vapor Permeability analyzer, equipped with two sensors (Extra solution, Perm tech, Italy), was used to measure and record the oxygen and water vapor transmission rates (OTR and WVTR, respectively) through films at a temperature of 23°C with an exposed area of $50\,cm^2$. The OTR and WVTR were defined as the flux $J(t)$ of oxygen and water vapor, respectively, transported per unit of time through the surface of the tested film at a specific temperature and relative humidity [69, 70]. For OTR measurements, the conditions were relative humidity (RH) of 65%, with an O_2 pressure of 1.5 bar and N_2 pressure of 2 bar. For WVTR measurements, the conditions were RH 100% and N_2 pressure of 2 bar. During permeability testing, the air-exposed side was oriented toward the upstream gas chamber, while the glass-contact side faced the downstream sensors.

4.4.5 | Water Contact Angle Measurement

The hydrophobicity of the unmodified and TER-modified EC films was evaluated using the Goniometer with First Ten Angstroms (FTA 1000) software (Newark, California, USA) equipped with a CCD camera using the sessile drop method with a droplet volume of 5 μL at lab-controlled room temperature (25°C). The static contact angle on the films was measured 30 s post-droplet deposition, allowing time for the droplet to stabilize and thereby minimizing variations attributable to initial spreading. The measurement was performed in triplicate, where the static contact angles were measured at five different positions for each sample, and average values were calculated.

To assess coating performance across all four substrates, the static contact angles were recorded for three distinct conditions—uncoated, unmodified EC, and TER-modified EC—using three independent replicates per group.

4.4.6 | UV Spectrophotometer

A transmittance test to assess the transparency of the coating material was conducted on the surface of a lab glass slide (2.5 × 2.5 cm) using a GENESIS 150 UV Spectrophotometer (Thermo Scientific, Waltham, MA, USA) over a 200–800 nm wavelength range.

4.4.7 | Statistical Analysis

All the characterization was conducted in triplicate to ensure reproducibility. Statistical analysis was performed using GraphPad Prism 8, with Microsoft Excel. The results are presented as arithmetic means ± standard deviations. Prior to analysis, datasets were assessed for parametric assumptions: the Shapiro–Wilk test was used for normality (Tables S1 and S2), and the Brown-Forsythe test was used for homogeneity of variance. Additionally, Spearman's rank correlation was employed to confirm the absence of heteroscedasticity ($p > 0.05$). For datasets satisfying these criteria, One-way ANOVA was used for single-variable comparisons, while Two-way ANOVA was applied to evaluate the interaction between multiple experimental factors. Statistical significance was determined at $p < 0.05$.

Acknowledgments

A.N. acknowledges financial support from the PON scholarship, funded by resources allocated by the MUR (Ministry of University and Research) under the Ministerial Decree for FSE resources REACT-EU, CUP: F85F21005880001, and from the University of Salento. A.S., C.D., and L.L. acknowledge the support of the PNRR–MUR for the funding allocated to Research Initiatives for Innovative Technologies and Pathways in Healthcare and Assistance (Decree No. 931, June 6, 2022), under the ANTHEM project (AdvaNced Technologies for HumancentEred Medicine), CUP B53C22006710001.

Funding

This work was supported by PON MUR, F85F21005880001 and PNRR MUR, B53C22006710001.

Conflicts of Interest

The authors declare no conflicts of interest.

Data Availability Statement

Data will be made available on request.

References

1. G. S. Nambafu, N. Kim, and J. Kim, "Hydrophobic Coatings Prepared Using Various Dipodal Silane-Functionalized Polymer Precursors," *Applied Surface Science Advances* 7 (2022): 100207.

2. D. Ahmad, I. van den Boogaert, J. Miller, R. Presswell, and H. Jouhara, "Hydrophilic and Hydrophobic Materials and Their Applications," *Energy Sources, Part A: Recovery, Utilization, and Environmental Effects* 40 (2018): 2686–2725.

3. L. Pérez-Gandarillas, D. Aragón, C. Manteca, et al., "Highly Hydrophobic Organic Coatings Based on Organopolysilazanes and Silica Nanoparticles: Evaluation of Environmental Degradation," *Coatings* 13 (2023): 537, https://doi.org/10.3390/coatings13030537.

4. M. Trapuzzano, N. B. Crane, R. Guldiken, and A. Tejada-Martínez, "Wetting Metamorphosis of Hydrophobic Fluoropolymer Coatings Submerged in Water and Ultrasonically Vibrated," *Journal of Coatings Technology and Research* 17 (2020): 633–642.

5. H. Huang, W. Wang, and L. Wang, "Theoretical Assessment of Wettability on Silane Coatings: From Hydrophilic to Hydrophobic," *Physical Chemistry Chemical Physics* 21 (2019): 8257–8263.

6. B. Améduri, "The Promising Future of Fluoropolymers," *Macromolecular Chemistry and Physics* 221 (2020): 1900573.

7. C. E. Pyo and J. H. Chang, "Hydrophobic Mesoporous Silica Particles Modified With Nonfluorinated Alkyl Silanes," *ACS Omega* 6 (2021): 16100–16109.

8. P. Cerny, P. Bartos, P. Kriz, P. Olsan, and P. Spatenka, "Highly Hydrophobic Organosilane-Functionalized Cellulose: A Promising Filler for Thermoplastic Composites," *Materials* 14 (2021): 2005, https://doi.org/10.3390/ma14082005.

9. K. Huang, A. Maltais, and Y. Wang, "Enhancing Water Resistance of Regenerated Cellulose Films With Organosilanes and Cellulose Nanocrystals for Food Packaging," *Carbohydrate Polymer Technologies and Applications* 6 (2023): 100391.

10. H. Liu, T. Zhou, X. Sun, and G. Zong, "Organosilane-Modified Wood Materials: A Review of Research and Applications," *BioResources* 18 (2023): 18.

11. K. M. Pieńkowska, *Concise Encyclopedia of High Performance Silicones* (Wiley, 2014), 243–251.

12. S. Roy and J. W. Rhim, "Advances and Challenges in Biopolymer-Based Films," *Polymers* 14 (2022): 3920.

13. L. Lamanna, G. Giacoia, M. Friuli, et al., "Oil-Water Emulsion Flocculation Through Chitosan Desolubilization Driven by pH Variation," *ACS Omega* 8 (2023): 20708–20713.

14. M. T. Ramesan, A. J. Kalladi, J. Mathew, K. Meera, S. Sankar, and M. Verma, "Reinforcement of Asparagus Racemosus as a Bio-Filler Agent in Polyvinyl Alcohol/Chitosan Blend for Flexible Electronic Devices Using a Green Approach," *Research on Chemical Intermediates* 50 (2024): 465–483.

15. M. T. Ramesan, A. J. Kalladi, A. C. Labeeba Abdulla, P. Sunojkumar, and B. K. Bahuleyan, "Development of Biopolymer Composite Films Based on Chicory Extract Reinforced Polyvinyl Alcohol/Chitosan Blend via Green Approach for Flexible Optoelectrical Devices," *Journal of Applied Polymer Science* 141 (2024): e55154.

16. M. Friuli, P. Nitti, L. Cafuero, et al., "Cellulose Acetate and Cardanol Based Seed Coating for Intraspecific Weeding Coupled With Natural Herbicide Spraying," *Journal of Polymers and the Environment* 28 (2020): 2893–2904.

17. S. Kopacic, A. Walzl, A. Zankel, et al., "Alginate and Chitosan as a Functional Barrier for Paper-Based Packaging Materials," *Coatings* 8 (2018): 235.

18. M. Mujtaba, J. Lipponen, M. Ojanen, S. Puttonen, and H. Vaittinen, "Trends and Challenges in the Development of Bio-Based Barrier Coating Materials for Paper/Cardboard Food Packaging; a Review," *Science of the Total Environment* 851 (2022): 158328.

19. U. Agarwal, A. Kumar, Z. Song, et al., "Transparent and Multifunctional Biocomposites for Sustainable Packaging Applications," *ACS Applied Polymer Materials* 7 (2024): 106–113.

20. J. Loste, J.-M. Lopez-Cuesta, L. Billon, H. Garay, and M. Save, "Transparent Polymer Nanocomposites: An Overview on Their Synthesis and Advanced Properties," *Progress in Polymer Science* 89 (2019): 133–158.

21. S. Guzman-Puyol, J. J. Benítez, and J. A. Heredia-Guerrero, "Transparency of Polymeric Food Packaging Materials," *Food Research International* 161 (2022): 111792.

22. L. Lamanna, "Recent Progress in Polymeric Flexible Surface Acoustic Wave Devices: Materials, Processing, and Applications," *Advanced Materials Technologies* 8 (2023): 2300362.

23. N. Asim, M. Badiei, and M. Mohammad, "Recent Advances in Cellulose-Based Hydrophobic Food Packaging," *Emergent Materials* 5 (2022): 703–718.

24. A. Narayanan, M. Friuli, A. Sannino, C. Demitri, and L. Lamanna, "Green Synthesis of Stretchable Ethyl Cellulose Film Plasticized With Transesterified Sunflower Oil," *Carbohydrate Polymer Technologies and Applications* 6 (2023): 100378.

25. A. N. M. A. Haque and M. Naebe, "Flexible Water-Resistant Semi-Transparent Cotton Gin Trash/Poly (Vinyl Alcohol) Bio-Plastic for Packaging Application: Effect of Plasticisers on Physicochemical Properties," *Journal of Cleaner Production* 303 (2021): 126983.

26. M. D. Hosen, M. S. Hossain, M. A. Islam, A. N. M. A. Haque, and M. Naebe, "Utilisation of Natural Wastes: Water-Resistant Semi-Transparent Paper for Food Packaging," *Journal of Cleaner Production* 364 (2022): 132665.

27. S. Zhang, J. Zhou, Y. Zhang, Y. Bi, and J. Li, "Preparation and Characteristics of Zein/Ethyl Cellulose Composite Coating Applied in Aqueous System," *International Journal of Biological Macromolecules* 282 (2024): 137274.

28. H. Chen, Z. Zhou, B. Zheng, et al., "Development and Characterization of Biodegradable Water- and Oil-Resistant Coatings Based on Derivatized Cellulose, Sodium Alginate, and Shellac for Paper-Based Packaging," *International Journal of Biological Macromolecules* 303 (2025): 140490.

29. Y. Wang, H. Zhang, L. Lin, et al., "Modification of Cellulose by Hydrophobic Long-Chain Molecules: Advances and Prospects," *Paper and Biomaterials* 5 (2020).

30. N. A. Belov, A. Y. Alentiev, Y. G. Bogdanova, A. Y. Vdovichenko, and D. S. Pashkevich, "Direct Fluorination as Method of Improvement of Operational Properties of Polymeric Materials," *Polymers* 12 (2020): 12, https://doi.org/10.3390/polym12122836.

31. F. Huang, X. Wu, Y. Yu, Y. Lu, and Q. Chen, "Acylation of Cellulose Nanocrystals With Acids/Trifluoroacetic Anhydride and Properties of Films From Esters of CNCs," *Carbohydrate Polymers* 155 (2017): 525–534.

32. L. Lamanna, G. Corigliano, A. Narayanan, et al., "Beyond Plastic: Oleogel as Gel-State Biodegradable Thermoplastics," *Chemical Engineering Journal* 498 (2024): 154988.

33. M. Friuli, A. Sannino, C. Demitri, and L. Lamanna, "Sustainable Alternatives to Silicone in Pest Management: A Comparative Study of Biodegradable Oleogel Pheromone Dispensers for *Plodia interpunctella*," *ACS Agricultural Science and Technology* 5 (2025): 138–141.

34. P. T. Le and K. T. Nguyen, "Hydrophobizing Cellulose Surfaces via Catalyzed Transesterification Reaction Using Soybean Oil and Starch," *Heliyon* 6 (2020): e05559.

35. X. Dong, Y. Dong, M. Jiang, L. Wang, J. Tong, and J. Zhou, "Modification of Microcrystalline Cellulose by Using Soybean Oil for Surface Hydrophobization," *Industrial Crops and Products* 46 (2013): 301–303.

36. X. Cao, S. Sun, X. Peng, L. Zhong, R. Sun, and D. Jiang, "Rapid Synthesis of Cellulose Esters by Transesterification of Cellulose With Vinyl Esters Under the Catalysis of NaOH or KOH in DMSO," *Journal of Agricultural and Food Chemistry* 61 (2013): 2489–2495.

37. U. Schuchardt, R. Sercheli, and R. M. Vargas, "Transesterification of Vegetable Oils: A Review," *Journal of the Brazilian Chemical Society* 9 (1998): 199–210.

38. M. E. Kibar, L. Hilal, B. T. Çapa, B. Bahçıvanlar, and B. B. Abdeljelil, "Assessment of Homogeneous and Heterogeneous Catalysts in Transesterification Reaction: A Mini Review," *ChemBioEng Reviews* 10 (2023): 412–422.

39. R. Sharma, K. H. Putera, M. M. Banaszak Holl, G. Garnier, and V. S. Haritos, "Modulating the Hydrophobicity of Cellulose by Lipase-Catalyzed Transesterification," *International Journal of Biological Macromolecules* 254 (2024): 127972.

40. R. Esposito, M. Melchiorre, A. Annunziata, M. E. Cucciolito, and F. Ruffo, "Emerging Catalysis in Biomass Valorisation: Simple Zn(II) Catalysts for Fatty Acids Esterification and Transesterification," *ChemCatChem* 12 (2020): 5858–5879.

41. F. D'Acierno and I. Capron, "Modulation of Surface Properties of Cellulose Nanocrystals Through Adsorption of Tannic Acid and Alkyl Cellulose Derivatives," *Carbohydrate Polymers* 319 (2023): 121159.

42. T. A. Dankovich and Y.-L. Hsieh, "Surface Modification of Cellulose With Plant Triglycerides for Hydrophobicity," *Cellulose* 14 (2007): 469–480.

43. J. Pullen and K. Saeed, "Investigation of the Factors Affecting the Progress of Base-Catalyzed Transesterification of Rapeseed Oil to Biodiesel FAME," *Fuel Processing Technology* 130 (2015): 127–135.

44. K. N. Onwukamike, S. Grelier, E. Grau, H. Cramail, and M. A. R. Meier, "Sustainable Transesterification of Cellulose With High Oleic Sunflower Oil in a DBU-CO2Switchable Solvent," *ACS Sustainable Chemistry and Engineering* 6 (2018): 8826–8835.

45. T. Kulomaa, J. Matikainen, P. Karhunen, M. Heikkilä, J. Fiskari, and I. Kilpeläinen, "Cellulose Fatty Acid Esters as Sustainable Film Materials – Effect of Side Chain Structure on Barrier and Mechanical Properties," *RSC Advances* 5 (2015): 80702–80708.

46. H. C. Erythropel, J. B. Zimmerman, T. M. de Winter, et al., "The Green ChemisTREE: 20 Years After Taking Root With the 12 Principles," *Green Chemistry* 20 (2018): 1929–1961.

47. A. Ivanković, A. Dronjić, A. M. Bevanda, and S. Talić, "Review of 12 Principles of Green Chemistry in Practice," *International Journal of Sustainable and Green Energy* 6 (2017): 39–48.

48. A. B. D. Nandiyanto, R. Oktiani, and R. Ragadhita, "How to Read and Interpret FTIR Spectroscope of Organic Material," *Indonesian Journal of Science and Technology* 4 (2019): 97–118.

49. A. Dutta, "Fourier Transform Infrared Spectroscopy," in *Spectroscopic Methods for Nanomaterials Characterization*, ed. S. Thomas, R. Thomas, A. K. Zachariah, and R. K. Mishra (Elsevier, 2017), 73–93.

50. W. Urbaniak-Domagala, "The Use of the Spectrometric Technique FTIR-ATR to Examine the Polymers Surface," *Advanced Aspects of Spectroscopy* 3 (2012): 85–104.

51. M. E. Di Pietro, A. Mannu, and A. Mele, "NMR Determination of Free Fatty Acids in Vegetable Oils," *PRO* 8 (2020): 410, https://doi.org/10.3390/pr8040410.

52. O. Awogbemi, E. I. Onuh, and F. L. Inambao, "Comparative Study of Properties and Fatty Acid Composition of Some Neat Vegetable Oils and Waste Cooking Oils," *International Journal of Low-Carbon Technologies* 14 (2019): 417–425.

53. A. C. Rustan and C. A. Drevon, "Fatty Acids: Structures and Properties," *Encyclopedia of Life Sciences* 1 (2005): 1–7.

54. H. M. Roche, "Unsaturated Fatty Acids," *Proceedings of the Nutrition Society* 58 (1999): 397–401.

55. A. Gopinath, K. Sairam, R. Velraj, and G. Kumaresan, "Effects of the Properties and the Structural Configurations of Fatty Acid Methyl Esters on the Properties of Biodiesel Fuel: A Review," *Proceedings of the Institution of Mechanical Engineers, Part D: Journal of Automobile Engineering* 229 (2015): 357–390.

56. J. d. A. Rodrigues, Jr., F. d. P. Cardoso, E. R. Lachter, L. R. M. Estevão, E. Lima, and R. S. V. Nascimento, "Correlating Chemical Structure and Physical Properties of Vegetable Oil Esters," *Journal of the American Oil Chemists' Society* 83 (2006): 353–357.

57. V. Kostik, S. Memeti, and B. Bauer, "Fatty Acid Composition of Edible Oils and Fats," *Journal of Hygienic Engineering and Design* 4 (2013): 112–116.

58. K. Chowdhury, L. A. Banu, S. Khan, and A. Latif, "Studies on the Fatty Acid Composition of Edible Oil," *Bangladesh Journal of Scientific and Industrial Research* 42 (2008): 311–316.

59. X. Su, Z. Yang, K. B. Tan, J. Chen, J. Huang, and Q. Li, "Preparation and Characterization of Ethyl Cellulose Film Modified With Capsaicin," *Carbohydrate Polymers* 241 (2020): 116259.

60. H. Mashhadi, A. Nourabi, M. Mohammadi, M. Tabibiazar, A. V. Farahani, and J. M. Lorenzo, "Incorporation of Myrtle Essential Oil Into Hydrolyzed Ethyl Cellulose Films for Enhanced Antimicrobial Packaging Applications," *Food Bioscience* 62 (2024): 105029.

61. J. M. Lagaron, R. Catalá, and R. Gavara, "Structural Characteristics Defining High Barrier Properties in Polymeric Materials," *Materials Science and Technology* 20 (2004): 1–7.

62. B. M. Trinh, B. P. Chang, and T. H. Mekonnen, "The Barrier Properties of Sustainable Multiphase and Multicomponent Packaging Materials: A Review," *Progress in Materials Science* 133 (2023): 101071.

63. S. H. Lee, Z. Ashaari, W. C. Lum, et al., "Thermal Treatment of Wood Using Vegetable Oils: A Review," *Construction and Building Materials* 181 (2018): 408–419.

64. P. Baumeister and G. Pincus, "Optical Interference Coatings," *Scientific American* 223 (1970): 58–75.

65. L. Lamanna, G. Pace, I. K. Ilic, et al., "Edible Cellulose-Based Conductive Composites for Triboelectric Nanogenerators and Supercapacitors," *Nano Energy* 108 (2023): 108168.

66. J. Wilkinson, C. Tam, A. Askounis, and S. Qi, "Suppression of the Coffee-Ring Effect by Tailoring the Viscosity of Pharmaceutical Sessile Drops," *Colloids and Surfaces A: Physicochemical and Engineering Aspects* 614 (2021): 126144.

67. W. S. M. Rathnayake, L. Karunanayake, A. M. P. B. Samarasekara, and D. A. S. Amarasinghe, "Sunflower Oil-Based MCC Surface Modification to Achieve Improved Thermomechanical Properties of a Polypropylene Composite," *Cellulose* 27 (2020): 4355–4371.

68. T. C. Mokhena and M. J. John, "Esterified Cellulose Nanofibres From Saw Dust Using Vegetable Oil," *International Journal of Biological Macromolecules* 148 (2020): 1109–1117.

69. R. Turco, R. Ortega-Toro, R. Tesser, et al., "Poly (Lactic Acid)/thermoplastic Starch Films: Effect of Cardoon Seed Epoxidized Oil on Their Chemicophysical, Mechanical, and Barrier Properties," *Coatings* 9 (2019): 574, https://doi.org/10.3390/coatings9090574.

70. A. Amior, H. Satha, A. Vitale, R. Bongiovanni, and S. Dalle Vacche, "Photocured Composite Films With Microfibrillated Cellulose: A Study of Water Vapor Permeability," *Coatings* 13 (2023): 297, https://doi.org/10.3390/coatings13020297.

Supporting Information

Additional supporting information can be found online in the Supporting Information section. **FIGURE S1:** The relative transesterification rate (R_{TER}) of the reaction between ethyl cellulose (EC) and fatty acid ethyl esters (FAEEs) of different vegetable oils, particularly peanut oil, soybean oil, and sunflower oil, at 110°C for different heat treatment times (0–240 min). **Figure S2:** Statistical analysis on the relative transesterification rate (R_{TER}) of ethyl cellulose reacted with fatty acid ethyl esters derived from peanut, soybean, and sunflower oils at 110°C. Data are presented across four reaction durations: (A) 30 min, (B) 60 min, (C) 90 min, and (D) 120 min. **Table S1:** The *p* values from the Shapiro–Wilk test for the relative transesterification rate, calculated for the reaction between ethyl cellulose and fatty acid ethyl esters of different vegetable oils (peanut oil, soybean oil, and sunflower oil) at 110°C for different time intervals: 30, 60, 90, and 120 min. **Table S2:** The *p* values from the Shapiro–Wilk test of unmodified EC and TER-modified EC for each experimental group of characterization.